BJCP British Journal of Clinical Pharmacology

DOI:10.1111/j.1365-2125.2011.04109.x

Mechanism-based population modelling of the effects of vildagliptin on GLP-1, glucose and insulin in patients with type 2 diabetes

Cornelia B. Landersdorfer,[1,2] Yan-Ling He[3] & William J. Jusko[1]

[1]Department of Pharmaceutical Sciences, State University of New York at Buffalo, Buffalo, NY, USA, [2]Centre for Medicine Use and Safety, Faculty of Pharmacy and Pharmaceutical Sciences, Monash University, Melbourne, VIC, Australia and [3]Translational Science-Translational Medicine, Novartis Institutes for BioMedical Research, Cambridge, MA, USA

Correspondence
William J. Jusko PhD, Department of Pharmaceutical Sciences, State University of New York at Buffalo, Buffalo, NY 14260, USA.
Tel.: +716 645 2855
Fax: +716 645 3693
E-mail: wjjusko@buffalo.edu

Part of this work has been presented as posters at the NIH Workshop on Quantitative and Systems Pharmacology, Bethesda, MD; September 25–26, 2008 and the American Conference of Pharmacometrics (ACoP), Mashantucket, CT; October 4–7, 2009. The data without modelling analysis have been published in: He Y-L *et al*. Clin Pharmacokinet 2007; 46: 577–588.

Keywords
GLP-1, glucose, insulin, mechanism-based population modelling, type 2 diabetes mellitus, vildagliptin

Received
1 December 2010

Accepted
14 September 2011

Accepted Article Published Online
10 October 2011

WHAT IS ALREADY KNOWN ABOUT THIS SUBJECT

- Vildagliptin is a potent and selective inhibitor of dipeptidylpeptidase-IV (DPP-4).
- DPP-4 inhibition leads to increased active glucagon-like peptide 1 (GLP-1) concentrations and decreased plasma glucose in patients with type 2 diabetes.

WHAT THIS STUDY ADDS

- No mechanism-based population PD modelling has been conducted to understand the effects of vildagliptin on active GLP-1, glucose and insulin.
- Active GLP-1 concentrations could be described by secretion of active GLP-1 from the gut in response to a meal and elimination by DPP-4 and an additional non-saturable elimination pathway.
- The effects of vildagliptin on glucose and insulin are primarily via enhanced GLP-1 concentrations which could be modelled by its effects on insulin secretion and peripheral insulin sensitivity.
- Parallelized S-ADAPT but not NONMEM VI proved to be an excellent choice for estimating a complex population model such as the current PK/PD model.

AIM

To build a mechanism-based population pharmacodynamic model to describe and predict the time course of active GLP-1, glucose and insulin in type 2 diabetic patients after treatment with various doses of vildagliptin.

METHODS

Vildagliptin concentrations, DPP-4 activity, active GLP-1, glucose and insulin concentrations from 13 type 2 diabetic patients after oral vildagliptin doses of 10, 25 or 100 mg and placebo twice daily for 28 days were co-modelled. The population PK/PD model was developed utilizing the MC-PEM algorithm in parallelized S-ADAPT version 1.56.

RESULTS

In the PD model, active GLP-1 production was stimulated by gastrointestinal intake of nutrients. Active GLP-1 was primarily metabolized by DPP-4 and an additional non-saturable pathway. Increased plasma glucose stimulated secretion of insulin which stimulated utilization of glucose. Active GLP-1 stimulated both glucose-dependent insulin secretion and insulin-dependent glucose utilization. Complete inhibition of DPP-4 resulted in an approximately 2.5-fold increase of active GLP-1 half-life.

CONCLUSIONS

The effects of vildagliptin in patients with type 2 diabetes on several PD endpoints were successfully described by the proposed model. The mechanisms of vildagliptin on glycaemic control could be evaluated from a variety of aspects such as effects of DPP-4 on GLP-1, effects of GLP-1 on insulin secretion and effects on hepatic and peripheral insulin sensitivity. The present model can be used to predict the effects of other dosage regimens of vildagliptin on DPP-4 inhibition, active GLP-1, glucose and insulin concentrations, or can be modified and applied to other incretin-related anti-diabetes therapies.

Introduction

Vildagliptin is a potent and selective inhibitor of dipeptidyl peptidase IV (DPP-4), leading to increased concentrations of active glucagon-like peptide 1 (GLP-1) and thereby decreased plasma glucose concentrations. Vildagliptin is approved for treatment of type 2 diabetes mellitus in more than 76 countries including the European Union and Japan where 85 to 95% of all diabetes cases are type 2 [1]. Such patients exhibit insufficient insulin activity due to decreased insulin action in glucose-utilizing tissues (peripheral insulin resistance) and impaired insulin secretion from the β-cells in the pancreas (β-cell failure).

After ingestion of a meal, GLP-1, an incretin hormone, is released from the L-cells in the gut wall. Its secretion is stimulated both by endocrine and neural signals and by direct stimulation of the intestinal cells by digested nutrients in the gut. Active GLP-1 stimulates glucose-dependent insulin secretion from β-cells, enhances β-cell proliferation and increases β-cell resistance to apoptosis [2]. GLP-1 has also been demonstrated to suppress hepatic glucose production and delay gastric emptying [3], thereby decreasing high blood glucose concentrations after food intake. GLP-1 is rapidly inactivated by the ubiquitous enzyme DPP-4 with a half-life of approximately 2 min in humans. Reduced secretion of GLP-1 in type 2 diabetic patients compared with healthy subjects has been reported [4, 5]. Vildagliptin, a DPP-4 inhibitor, prolongs the action of active GLP-1 by inhibiting its inactivation by the DPP-4 enzyme.

While the effects of vildagliptin from this study in type 2 diabetic patients were previously described by non-compartmental analysis (NCA) [6], a mechanism-based compartmental modelling approach has not been applied. Simultaneous modelling of PD endpoints such as DPP-4, GLP-1, insulin and glucose by taking the pathophysiology into account allows the exploration of the dynamic aspects of mechanisms of action and the interactions between these PD endpoints when vildagliptin intervenes. In addition the population approach takes into account the variability between patients and adequately considers measurements below the quantification limit. Utilizing parallelized S-ADAPT with the Monte Carlo parametric expectation maximization (MC-PEM) algorithm, a state-of-the-art algorithm which calculates the exact log likelihood, allows the estimation of the whole system by a full population approach which was not possible in NONMEM.

Our companion article describes a mechanism-based population model that simultaneously captures the PK of vildagliptin and its effects on DPP-4 activity in type 2 diabetic patients at different dose levels [7]. In the present report, we further developed a mechanism-based PK/PD model including downstream PD endpoints of GLP-1, insulin and glucose based on our PK/DPP-4 model to understand further the dynamics of the mechanism of action of vildagliptin.

The overall aim of our study was to develop a mechanism-based population PK/PD model that simultaneously describes vildagliptin PK, inhibition of DPP-4 activity and changes in active GLP-1, glucose and insulin at different dose levels based on the mechanism of action of vildagliptin.

Methods

A detailed report on the clinical and bioanalytical procedures that are not described here was published [6]. A brief description is provided in the companion article [7].

Study participants

Thirteen adult patients who had been diagnosed with type 2 diabetes for at least 3 months prior to screening were included in the study. A washout period from hypoglycaemic drugs of up to 4 weeks was required. The study was approved by the local ethics committee and conducted in full compliance with the Declaration of Helsinki. All patients signed written informed consent.

Study design and drug administration

The study was a randomized, placebo-controlled, double-blind, four-way crossover trial. The subjects received twice daily oral doses of 10, 25 or 100 mg vildagliptin (Galvus™) and placebo as tablets for 28 days. Patients were at the study site on day 1 and from the evening of day 26 to the morning of day 29 in each study period. During the confinement periods the patients received a standard diet with identical meals for all four treatments. Breakfast and dinner were consumed at approximately 30 min after the doses. The duration of food intake was reported for each individual patient and meal.

Sampling schedule and bioanalysis

Blood samples for measurement of active GLP-1, glucose and insulin concentrations were obtained on day 28 of each treatment period. Samples for GLP-1 were taken predose and at 0.5, 0.58, 0.67, 0.75, 1, 1.5, 2, 3, 5, 8, 10.5, 10.58, 10.67 10.75, 11, 11.5, 12, 14 and 16 h after the morning dose. Blood samples for determination of glucose and insulin were collected prior to dosing and at 0.75, 1, 1.25, 1.5, 2, 2.5, 3, 4, 5, 5.5, 5.75, 6, 6.5, 7, 8, 9.75, 10.25, 10.75, 11, 11.25, 11.5, 12, 12.5, 13 and 14 h after the morning dose. All samples were centrifuged and plasma was frozen at –70°C or lower until analysis.

Active GLP-1 in plasma was determined utilizing the GLP-1 (active) ELISA kit (Linco Research, Inc., St. Charles, MO, USA). The lower limit of quantification (LLQ) was 2 pmol l^{-1}. The glucose assay was performed on a Hitachi 747–200 Autoanalyzer (Roche Diagnostics, Indianapolis, IN, USA) and had a linear range up to 750 mg dl^{-1}. Insulin was

measured by electrochemiluminescence on a 2010 Elecsys System (Roche Diagnostics) with an LLQ of 0.2 mIU ml^{-1}.

Non-compartmental analysis

The individual areas under the curve (AUC) for vildagliptin, active GLP-1, glucose and insulin were calculated using the linear up/log down (linear interpolation when concentrations are increasing, logarithmic interpolation for decreasing concentrations) as implemented in WinNonlin Pro version 5.0.1 (Pharsight Corporation, Mountain View, CA, USA).

Compartmental modelling

All GLP-1, glucose, and insulin profiles from the three different treatments and placebo were modelled simultaneously utilizing the MC-PEM algorithm in S-ADAPT version 1.56 [8] with the Beal M3 method for handling data below the limit of quantification [9]. Model discrimination was based on the following four criteria: 1) visual inspection of the observed and predicted profiles, 2) visual comparison of the patterns of systematic and random residuals, 3) the objective function and 4) visual predictive checks.

For the visual predictive checks, GLP-1, glucose and insulin concentration–time profiles were simulated for 5000 subjects for each competing model in S-ADAPT version 1.56. The median and non-parametric prediction intervals were calculated and compared with the observed data as described in the companion report. Ideally, the median should mirror the central tendency of the data and 20% of the observed data points should fall outside the 80% prediction interval over all time points.

Standard errors were obtained from the full PK/PD model by utilizing the type 1 bootstrap method (see S-ADAPT manual under heading poperr_type) as implemented in S-ADAPT [8] in order to obtain a measure for precision of parameter estimates. This method randomly selects sets of patients from the dataset. A number of 200 bootstrap runs was performed to obtain standard errors.

Population PK model

Details on the PK model are provided in the companion article [7]. Briefly, the vildagliptin PK and DPP-4 activity were described simultaneously by a model for target-mediated drug disposition (TMDD), which accounts for the high affinity capacity-limited binding of vildagliptin to DPP-4 in both plasma and tissues. The model assumes that after the drug-enzyme complex has been formed, a fraction of the vildagliptin molecules is hydrolyzed by DPP-4.

Structural PD model

The diagram of the full structural PD model is illustrated in Figure 1. First the active GLP-1 concentrations were included in the previously developed model for vildagliptin PK and DPP-4 activity. Active GLP-1 secretion is stimulated by the presence of glucose in the gut. The amounts of glucose in the gut after breakfast, lunch, dinner and snack

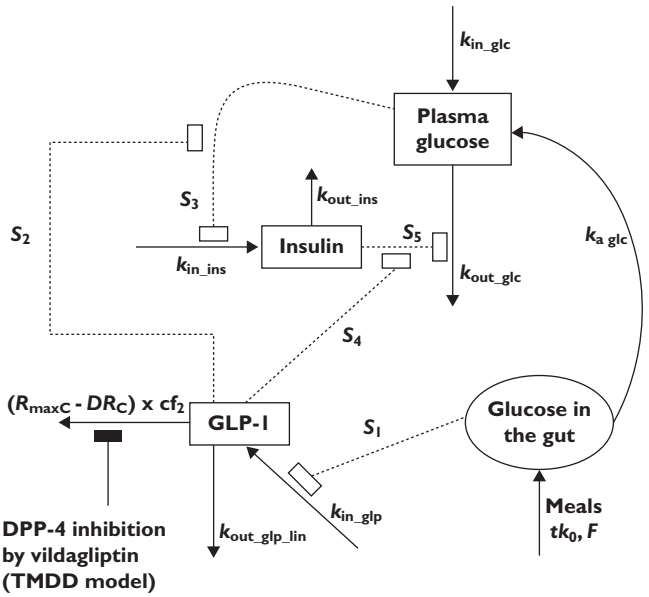

Figure 1
Model diagram. Symbols are defined in the text and in Table 1

were modelled by assuming an arbitrary value of 75000 mg glucose for each meal and then estimating glucose bioavailability from the meal by which the input was multiplied. Different glucose bioavailabilities, and therefore different amounts of glucose absorbed, were estimated for each type of meal to account for the different amounts of glucose absorbed after breakfast (75 g $\times$ F_B), lunch (75 g $\times$ F_L), dinner (75 g $\times$ F_D) and snack (75 g $\times$ F_S), as described below. As the meals were standardized throughout all study periods and no between treatment period variability was applied, the four different bioavailabilities could be estimated. The input of glucose (as food) into the gut compartment was modelled as a zero-order process with the duration (tk_0) being the actual recorded duration of food intake for each individual patient and each meal. The amounts of glucose in the gut (mg) after breakfast (A_{GB}), lunch (A_{GL}), dinner (A_{GD}) and snack (A_{GS}) were

$$\frac{dA_{GB}}{dt} = \text{Input} \times F_B - k_{aB} \times A_{GB}$$

$$\frac{dA_{GL}}{dt} = \text{Input} \times F_L - k_{aL} \times A_{GL}$$

$$\frac{dA_{GD}}{dt} = \text{Input} \times F_D - k_{aD} \times A_{GD}$$

$$\frac{dA_{GS}}{dt} = \text{Input} \times F_S - k_{aS} \times A_{GS}$$

where k_{aB}, k_{aL}, k_{aD} and k_{aS} (h^{-1}) are the first order absorption rate constants after breakfast, lunch, dinner and snack. The F_B, F_L, F_D and F_S are factors for the estimation of the total

amounts of glucose absorbed after ingestion of the corresponding meals. All initial conditions were zero. Input (mg h^{-1}) is the rate of glucose input into the gut compartment calculated as

$$\frac{75000\,(\text{mg glucose})}{\text{Individual duration of food intake}\,(\text{h})}$$

The total amount of glucose in the gut compartment (Glc_{gut}, mg) was

$$Glc_{Gut} = A_{GB} + A_{GL} + A_{GD} + A_{GS}$$

The concentration of active GLP-1 in plasma (C_{glp}, pM) was

$$\frac{dC_{glp}}{dt} = k_{in\_glp} \times (1 + S_1 \times Glc_{Gut}) - [k_{out\_glp\_lin} + (R_{maxC} - DR_C) \times cf_2] \times C_{glp}$$

where k_{in_glp} (pM h^{-1}) was the rate of active GLP-1 secretion at baseline, i.e. in the fasting state, and $k_{out\_glp\_lin}$ (h^{-1}) was the first-order elimination rate constant for active GLP-1 eliminated by a non-saturable pathway. The elimination of GLP-1 by DPP-4 was saturable and described by $(R_{maxC} - DR_C \times cf_2$, as explained below. The initial condition was the active GLP-1 concentration at baseline (B_{glp}).

The extent of stimulation of active GLP-1 secretion was assumed to be proportional to the total amount of glucose in the gut (Glc_{gut}, mg) which was changing over time and S_1 (mg^{-1}) was the proportionality factor. The ($R_{maxC} - DR_C$) described the amount of free DPP-4 enzyme in plasma changing over time, calculated as the difference between the amount of total DPP-4 (DPP-4 available for binding of vildagliptin at zero concentration of vildagliptin) and the amount of the DPP-4-vildagliptin complex. The ($R_{maxC} - DR_C$) denotes the free DPP-4 enzyme and comes from the PK model for vildagliptin and DPP-4 described in the companion article [7]. The rate of elimination of active GLP-1 by DPP-4 changed over time and was proportional to the amount of free DPP-4 in plasma (nmol) with cf_2 (h^{-1} $nmol^{-1}$) as the proportionality factor. The steady-state condition was

$$k_{in\_glp} = B_{glp} \times (k_{out\_glp\_lin} + R_{maxC} \times cf_2)$$

The GLP-1 model parameters were estimated simultaneously with the equations for vildagliptin PK and DPP-4 activity described in the companion article [7]. Then the equations for glucose and insulin were added.

The glucose absorption rate from the gut compartment was

$$Glc_{GutAb} = \frac{k_{aB} \times A_{GB} + k_{aL} \times A_{GL} + k_{aD} \times A_{GD} + k_{aS} \times A_{GS}}{V_{glc}}$$

where V_{glc} (dl) is the volume of distribution of glucose.

The glucose concentration in plasma (C_{glc}) was

$$\frac{dC_{glc}}{dt} = k_{in\_glc} + Glc_{GutAb} - k_{out\_glc} \times [1 + ST_{ins} \times (C_{ins} - B_{ins})] \times C_{glc}$$

where k_{in_glc} (mg dl^{-1} h^{-1}) is the endogenous production rate of glucose, k_{out_glc} (h^{-1}) is the first-order rate constant of glucose elimination, C_{ins} (mIU l^{-1}) is insulin concentration, and B_{ins} is insulin concentration at baseline. The initial condition is the glucose concentration at baseline (B_{glc}). The steady-state condition was

$$k_{in\_glc} = B_{glc} \times k_{out\_glc}$$

The ST_{ins} (l mIU^{-1}) describes the extent of stimulation of glucose utilization by insulin concentrations above baseline ($C_{ins} - B_{ins}$) and therefore is a measure of peripheral insulin sensitivity based on the model described here. The ST_{ins} value depends on the GLP-1 concentration (C_{glp}):

$$ST_{ins} = S_5 \times [1 + S_4 \times (C_{glp} - B_{glp})]$$

where S_5 (l mIU^{-1}) is the stimulation factor for glucose utilization by insulin when GLP-1 concentrations are at baseline ($C_{glp} = B_{glp}$). The proportionality factor S_4 (l $pmol^{-1}$) describes the increase of peripheral insulin sensitivity by active GLP-1 concentrations above baseline ($C_{glp} > B_{glp}$), i.e. the same concentration of insulin has a larger effect on glucose utilization when GLP-1 concentrations are increased compared with when GLP-1 concentrations are low.

The concentration of insulin in plasma (mIU l^{-1}) was

$$\frac{dC_{ins}}{dt} = k_{in\_ins} \times [1 + ST_{glc} \times (C_{glc} - B_{glc})] - k_{out\_ins} \times C_{ins}$$

where k_{in_ins} (mIU l^{-1} h^{-1}) is the endogenous production rate of insulin and k_{out_ins} (h^{-1}) is the first order rate constant for insulin elimination. The initial condition is the insulin concentration at baseline (B_{ins}). The steady-state condition was

$$k_{in\_ins} = B_{ins} \times k_{out\_ins}$$

The ST_{glc} (dl mg^{-1}) describes the extent of stimulation of insulin secretion by glucose concentrations above baseline which is enhanced by active GLP-1

$$ST_{glc} = S_3 \times [1 + S_2 \times (C_{glp} - B_{glp})]$$

where S_3 (dl mg^{-1}) is the stimulation factor for insulin secretion by glucose when GLP-1 concentrations are at baseline. The proportionality factor S_2 (l $pmol^{-1}$) describes the increase of pancreatic glucose sensitivity by active GLP-1 concentrations above baseline.

In the full PK/PD model all PK (shown in the companion report [7]) and PD parameters were estimated at the same time.

Individual PD model

Between subject variability (BSV) was included for all estimated PD parameters. A log-normal distribution was assumed and a full variance-covariance matrix for the BD

parameters was included. A full variance-covariance matrix was also implemented for the PK parameters. No covariance was included between PK and PD parameters. S-ADAPT estimates the BSV as variance. The square root of the variance is reported for BSV, as this is an approximation to the apparent coefficient of variation of a normal distribution on log-scale. Between occasion variability was not included.

Observation model

The residual unidentified variability was described by a combined additive and proportional error model for active GLP-1, glucose and insulin concentrations.

Results

All four periods of the study were completed by 12 subjects and one patient completed only the treatments with 10 and 25 mg vildagliptin. The average (range) weight of the subjects was 91 (65–116) kg, height 166 (148–183) cm and age 53.5 (37–64) years. Seven patients were female and six were male.

The observed concentrations of active GLP-1, glucose and insulin from all individual subjects and for all study periods are shown in Figures 2 to 4. Plots of the individual profiles of active GLP-1, glucose and insulin (not shown here) revealed a relatively high variability between the patients with various degrees of type 2 diabetes. *Post hoc* fits for one subject and two different doses of vildagliptin are shown in Figure 5.

The individual ratios of $AUC_{treated} : AUC_{placebo}$ for GLP-1, glucose and insulin *vs*. the AUC of vildagliptin are presented in Figure 6. The AUC of active GLP-1 was higher during vildagliptin treatment than during placebo treatment and the $AUC_{treated} : AUC_{placebo}$ increased with increasing $AUC_{vildagliptin}$ for all subjects except one. At an $AUC_{vildagliptin}$ of 500 ng ml^{-1} h or larger, the individual $AUC_{glucose}$ values were lower than with placebo treatment for almost all subjects. Overall the $AUC_{treated} : AUC_{placebo}$ for glucose decreased with increasing $AUC_{vildagliptin}$. The $AUC_{treated} : AUC_{placebo}$ for insulin did not show a clear trend with increasing $AUC_{vildagliptin}$ as insulin concentrations and insulin AUC were similar among all treatments.

Mechanism-based compartmental modelling

The parameter estimates and their BSV are reported in Table 1. The inclusion of each of the main model features based on objective function differences and mechanistic reasons is substantiated in Table 2. The profiles of active GLP-1, glucose and insulin were described by one set of parameter estimates for all three doses of vildagliptin and placebo treatment. The parameters S_1 to S_5 are stimulation factors which are multiplied by the changing GLP-1, glucose or insulin concentrations and thereby describe their effects. The newly developed model includes the secretion of active GLP-1 which is stimulated by food intake and the elimination of active GLP-1 by saturable metabolism due to DPP-4 and an additional linear elimination pathway. Inclusion of the additional elimination pathway which is not saturable at the achieved GLP-1 concentrations was necessary to describe the profiles. The model suggests that, at complete inhibition of DPP-4 in plasma, the half-life of active GLP-1 in plasma was increased by approximately 2.5-fold compared with no inhibition of DPP-4. The half-life of active GLP-1 at complete DPP-4 inhibition was calculated from the estimate of $k_{out\_glp\_lin}$ and the half-life at 0% (absence) of DPP-4 inhibition was calculated from ($k_{out\_glp\_lin} + R_{maxC} \times cf_2$). The profiles of active GLP-1 elimination by DPP-4 (($R_{maxC} - DR_C$) $\times$ cf_2), expressed as a 'rate constant' which changes over time, are shown in Figure 7A. The GLP-1 elimination due to DPP-4 depends on the available free DPP-4 and therefore decreases with decreasing DPP-4 activity (see companion article [7], vildagliptin is both an inhibitor and substrate of DPP-4) after a vildagliptin dose and is constant for placebo treatment.

The model includes the reciprocal feedback between glucose and insulin with stimulation of insulin secretion by glucose (ST_{glc}) and stimulation of glucose utilization by insulin (ST_{ins}). These effects occur at baseline GLP-1 concentrations (where $ST_{glc} = S_3$ and $ST_{ins} = S_5$) and are increased at higher concentrations of GLP-1. The changes in ST_{glc} and ST_{ins} over time are depicted in Figure 7B, C. Both the stimulation of insulin secretion per concentration unit of glucose (ST_{glc}, l mg^{-1}) and stimulation of glucose utilization per concentration unit of insulin (ST_{ins}, l mIU^{-1}) depend on active GLP-1 concentration. Therefore ST_{glc} (Figure 7C) and ST_{ins} (Figure 7B) are increased when vildagliptin is given compared with placebo. The GLP-1 effect of increasing the stimulation of insulin secretion ($S_2 \times (C_{glp} - B_{glp})$) by glucose reflects an increase in pancreatic glucose sensitivity. The effect of GLP-1 on increasing the insulin-dependent glucose utilization ($S_4 \times (C_{glp} - B_{glp})$) describes enhanced peripheral insulin sensitivity due to GLP-1. Thereby the decrease in glucose concentrations with the higher vildagliptin doses despite similar insulin concentrations among treatments could be successfully described. Inclusion of both GLP-1 effects (S_2 and S_4) was necessary in order to describe adequately the data. Comparison of simulated glucose profiles when one of the two effects was set to zero suggests that the effect on peripheral insulin sensitivity (described by S_4) was slightly larger than the effect on pancreatic glucose sensitivity (described by S_2).

Insulin secretion (mIU l^{-1} h^{-1}) as predicted by the model from ($k_{in\_ins} \times (1 + ST_{glc} \times (C_{glc} - B_{glc}))$) is shown in Figure 7D. Based on comparison of the profiles between placebo and the three different doses of vildagliptin the model suggests that insulin secretion was similar for all four treatments. The profiles for ST_{glc}, ST_{ins} and insulin secretion in Figure 7B, C and D suggest that the effect of vildagliptin

DOCKET ALARM

Explore Litigation Insights

Docket Alarm provides insights to develop a more informed litigation strategy and the peace of mind of knowing you're on top of things.

Real-Time Litigation Alerts

Keep your litigation team up-to-date with **real-time alerts** and advanced team management tools built for the enterprise, all while greatly reducing PACER spend.

Our comprehensive service means we can handle Federal, State, and Administrative courts across the country.

Advanced Docket Research

With over 230 million records, Docket Alarm's cloud-native docket research platform finds what other services can't. Coverage includes Federal, State, plus PTAB, TTAB, ITC and NLRB decisions, all in one place.

Identify arguments that have been successful in the past with full text, pinpoint searching. Link to case law cited within any court document via Fastcase.

Analytics At Your Fingertips

Learn what happened the last time a particular judge, opposing counsel or company faced cases similar to yours.

Advanced out-of-the-box PTAB and TTAB analytics are always at your fingertips.

API

Docket Alarm offers a powerful API (application programming interface) to developers that want to integrate case filings into their apps.

LAW FIRMS
Build custom dashboards for your attorneys and clients with live data direct from the court.

Automate many repetitive legal tasks like conflict checks, document management, and marketing.

FINANCIAL INSTITUTIONS
Litigation and bankruptcy checks for companies and debtors.

E-DISCOVERY AND LEGAL VENDORS
Sync your system to PACER to automate legal marketing.